Soft Matter

Accepted Manuscript

This is an *Accepted Manuscript*, which has been through the Royal Society of Chemistry peer review process and has been accepted for publication.

Accepted Manuscripts are published online shortly after acceptance, before technical editing, formatting and proof reading. Using this free service, authors can make their results available to the community, in citable form, before we publish the edited article. We will replace this *Accepted Manuscript* with the edited and formatted *Advance Article* as soon as it is available.

You can find more information about *Accepted Manuscripts* in the Information for Authors.

Please note that technical editing may introduce minor changes to the text and/or graphics, which may alter content. The journal's standard Terms & Conditions and the Ethical guidelines still apply. In no event shall the Royal Society of Chemistry be held responsible for any errors or omissions in this *Accepted Manuscript* or any consequences arising from the use of any information it contains.

ROYAL SOCIETY OF CHEMISTRY

www.rsc.org/softmatter

A Mutliscale Approach for Modeling Actuation Response of Polymeric Artificial Muscle

Soodabeh Sharafi[a], Guoqiang Li[a,b,*]

[a] Department of Mechanical & Industrial Engineering, Louisiana State University, Baton Rouge, LA 70803, USA
[b] Department of Mechanical Engineering, Southern University, Baton Rouge, LA 70813, USA

[*]Correspondence author: Tel.: 001-225-578-5302; Fax: 001-225-578-5924; E-mail: lguoqi1@lsu.edu

Abstract:

Artificial muscle is an emerging material in the field of smart materials with application in aerospace, robotic, and biomedical industries. Despite extensive experimental investigation in this field, there is a need for numerical modeling techniques that facilitate cutting edge research in this field. This work aims at studying an artificial muscle made of twisted Nylon 6.6 fibers that are highly cold-drawn. A computationally efficient phenomenological thermo-mechanical constitutive model is developed in which several physical properties of the artificial muscles are incorporated to minimize the trial-and-error numerical curve fitting processes. Two types of molecular chains are considered in micro-scale level that controls training and actuation processes viz. (a) helically oriented chains which are structural switches that store a twisted shape in their low temperature phase and restore their random configuration during thermal actuation process, and (b) entropic chains which are highly drawn chains that could actuate as soon as the muscle heats up, and saturates when coil contact temperature is reached. The thermal actuation response of the muscle over working temperatures has been elaborated in modeling section. The performance of the model is validated by available experiments in the literature. The model may provide a design platform for future artificial muscle developments.

Keywords: Artificial muscle; Constitutive modeling; Actuation; Fishing line.

1. Introduction

Man-made smart materials called artificial muscles are reversibly capable of extension, contraction or rotation, triggered by external stimuli such as chemical, electrical, pneumatic and thermal. Artificial muscles have become a popular topic of research in the past few years within the area of biomechanics, robotics, aerospace garment and many more. Pioneering designs comprise a vast category of materials based on four actuation mechanisms, including electric field actuations, ion-based diffusions, pressurized mechanisms and thermal actuations [1-6]. Bio-inspired designs and their structural change have been studied comprehensively. Zhao et al.[7] reviewed the recent methods for designing bio-inspired materials in which the systematic procedure for design, analysis and producing new materials is categorized and elaborated for biological materials. For example, in a study by Qin et al.[8], combination of theoretical and chemistry-based atomistic level model are utilized to study the effect of peptide length on the stability of alpha helix structure. The study focuses on physical mechanism that results in maximum stability of alpha-helix critical length. The critical length and probability distribution are two key concepts for understanding the folding mechanism and stability of alpha helix structure formation. However, the proposed modeling techniques do not consider macroscopic responses such as stress-strain relations or temperature effect on the evolution of helical structures. Liu et al. [9] provides a macroscopic analysis for the effects of geometry of rod structures on actuation response, which is the number of twist and structural transition under

Soft Matter Accepted Manuscript

tension, although the structural evolution under thermal loading and temperature effects are not considered. In another study by Qin et al.[10], the transition from α-helix to β-sheet as a common deformation mechanism in the α-helical rich proteins is studied. The length of α-helical coiled-coil proteins is a key factor in determination of α- β- transition, which affects the stiffness, strength and energy dissipation at large deformation. In this study the root cause of this type of transition in long α-helical protein structure is explained.

Some limitations of the previous muscles include short life cycle and loss of stored energy due to dissipative mechanisms mainly rooted in hysteresis cycle and low work efficiency. The popularity of the subject motivates researchers to fabricate new category of muscles with almost zero structural loss. Haines et.al.[11] introduced a new category of artificial muscles from low cost fishing lines or sewing threads. These muscles are working in a hysteresis-free actuation, which provide the highest efficiency compared to other kinds of artificial muscles. The enhanced muscle response is sourced in its reversible contraction in the microscopic structure, which has large volumetric thermal expansion and inhomogeneous dimensional change due to thermal actuation. The thermal actuation occurs within temperature fluctuations from room temperature to above glass transition temperature (T_g) and *vice versa.*

Because of the varying actuation mechanisms for artificial muscles, a number of studies have been conducted in the literature. One may mention models proposed to study electrochemical driven artificial muscles that link the macro mechanical behavior to the change in chemical components [2, 12]. In the case of electrochemical muscles, the ion diffusion and some mechanical and chemical reordering should be controlled which may add more complexity to the model. In the case of pneumatic muscles, fluid dynamics models have been developed in which state variables are space and time dependent, and moreover, the boundary conditions are time dependent [13]. Control based design approaches have also been used to capture high nonlinearity of pneumatic artificial muscles [3]. A two-state model is also developed to study force deflection variations in shape memory alloy [7] coiled spring actuator [14]. In the case of muscle made of shape memory Nitinol wire, a developed model works based on stress-strain-power relationship, which is applied to control underwater robotic movement [15].

While these models have been successful in modeling a specific category of muscles, they suffer from the large number of parameters that are needed to define the model behavior. Most importantly, the existing models do not address the newly developed polymer based artificial muscles, which is the subject of the current study.

In this work a phenomenological model has been developed based upon microstructural descriptions in which the muscle mainly comprises amorphous phase chains and the contribution by crystalline mircophases are negligible. Amorphous chains are subdivided into helically oriented chains and highly drawn chains. Specific types of deformation mechanisms are assumed for each helically oriented chain and highly drawn chain, to be responsible for actuation responses in various types of muscle structures. This paper is arranged as follows. In section 2, namely physics behind polymeric artificial muscles, the effect of microstructural engineering process and training cycles on the formation of the muscles is elaborated. Then, principle for thermal actuation responses in artificial muscle is discussed and the microscopic and macroscopic responses are developed. In section 3, model description, phenomenological model

Soft Matter Accepted Manuscript

and constitutive model are outlined and formulated. Modeling framework is defined in section 4 including mathematical modeling of actuation response of the muscle. Section 5 presents the numerical results.

2. Physical Characteristics

2.1 Microstructural Engineering and Training Cycles

Thermal actuation mechanism in polymeric artificial muscles is designed through a two-step engineering process, viz. microstructural engineering and training cycle. The microstructural engineering defines the shape of the muscle as well as the type of the actuation mechanisms, such as electro-chemical, etc. Different microstructures of polymer fibers have been examined by Haines et al.[11] as a precursor to produce the muscle, such as nylon 6, nylon 6.6, etc. The microstructures of these fibers need to be engineered in order to add actuation capabilities to the fibers. The microstructural design process includes (1) cold drawn tension that results in the so-called precursor fibers; and (2) twisting the precursor fibers. The final product from these nylon fibers is capable of actuation in response to external stimuli; and it is called artificial muscle hereinafter. Details regarding the fabrication process of the artificial muscles by twist insertion can be found in [11], and is outlined herein for sake of completeness.

There are two types of muscle fabrication method, coiling muscle by extra twisting of the precursor fiber and annealed muscle by annealing the twisted fiber around a mandrel. In the coiling method, the coiling is inserted by over-twisting. In the annealing process, the size of a mandrel defines the muscle's final geometry. The precursor fiber is twisted around mandrel to build spiral structure named muscle. Then the annealing process is set to fix the muscle's shape by raising the temperature to the melting point of the fiber. These methods result in different shape and load carrying response. The coiled muscle has lower stroke but higher load capability; the annealed muscle has higher stroke but lower load lifting capacity. From the microscopic point of view, the amount of helically oriented chains in the annealed muscle is less than that in the coiled muscle. Therefore, the annealing fabrication process produces muscles with lower load carrying ability and higher strain response.

The microstructure of the precursor fiber mostly consists of (a) amorphous phase, Gaussian chains that are highly oriented in the direction of cold strain; and (b) minor crystalline bridges, see Fig. 1a. These precursor fibers are famous for their high strength, enabling them to be used even as fishing lines. Fig. 1 schematically demonstrates the microstructural design process by microstructure engineering (Step 1). Both Fig. 1(a) and 1(b) show the first step in the micro structural engineering process. Fig. 1(a) shows the random distribution of the amorphous chains that are bridged by the crystalline phase before cold drawing. Fig. 1(b) illustrates the effect of cold drawing on the microstructure of the fiber in which highly drawn chains are produced in the direction of drawing. Fig. 1(c) depicts the effect of the twisting process in which helically oriented chains are produced due to the inelastic deformation mechanisms. The highly drawn and helically oriented polymer chains are capable of responding to external stimuli and the degree of stretch/twist governs the actuation efficiency of these smart muscles.

Soft Matter Accepted Manuscript

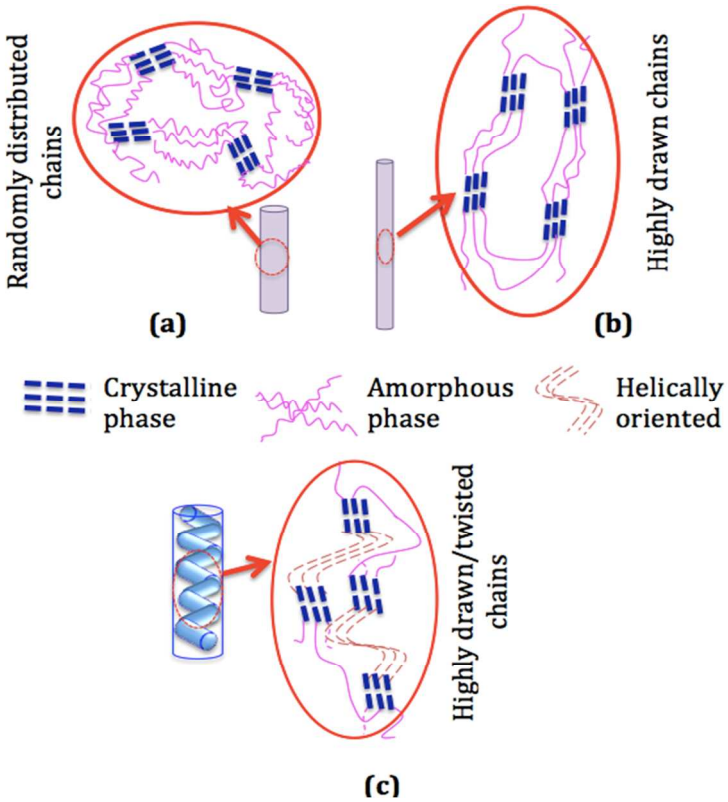

Fig.1 Schematic of the microstructure change in the engineering processes

In Step 2, training cycles are conducted. A muscle is trained in repetitive cycles to ensure a stable reversible actuation response with minimum hysteresis effects. The helically oriented chains resulting from Step 1 is trained in the loading-unloading cycles and it is reversible by changing temperature. This process of multiple heating and cooling cycle is designed to train thermally activated muscle until reversible actuation response is obtained. The heating process is initiated from room temperature with a very rapid cycle about 17 seconds up to above the glass transition temperature of the muscle. In each cycle the muscle shrinks when lifting loads by heating or expands while carrying load by cooling. In this step the reversible helical path of motion is established within the repetitive cycles. Training cycle between high (95^{o}C) and low temperatures (25^{o}C) as stated by Haines et al. [11]guarantees the actuation response in this muscle.

2.2 Principle of Thermal Actuation Responses

From the thermodynamics point of view, amorphous phases are less energetically stable comparing to crystalline phases. Consequently upon applying thermomechanical energies, amorphous chains undergo structural changes first while the crystalline phase remains intact.

Amorphous phase plays a dual role in thermal actuation responses in which the highly drawn chains behave like an entropic elastic chain that recovers their original shape upon unloading. For the helical chains, each helically oriented chain acts as a structural switch that twists or untwists over the actuation temperature range. Structural switches have two mechanisms that can be activated by temperature variation: relaxation mechanism that is activated during the cooling process and entropic mechanism that is turned on during the heating

Soft Matter Accepted Manuscript

process.

Fig. 2 shows the microstructural changes during the heating up process where the entropic mechanism enforces structural switches to move along the helical path; see Figs. 2(a) and 2(b). The accumulations of these helical motions result in fluctuation in the form of contraction/expansion in the draw direction. Upon saturation of contraction, the helically oriented chains start to intervene with each other, as shown in Fig. 2(c). Fig. 2(c) shows two helically oriented chains, which are intervening with each other and shrinking in the helical path; this motion resulting in radial expansion because there is no room for motion in the longitudinal direction. In other words, the anisotropy in thermal expansion starts playing a role and the extra heat expands muscle radially while inter-coiling process continues. The resulting motion swells muscle radially; see Fig. 2(c). During the cooling down process, *relaxation mechanisms* occur in which structural switches experience reverse motion along the helical path toward lower entropic levels. These relaxation mechanisms impel both structural switches and entropic chains (amorphous phase) to expand in the longitudinal direction upon regaining their low temperature configuration.

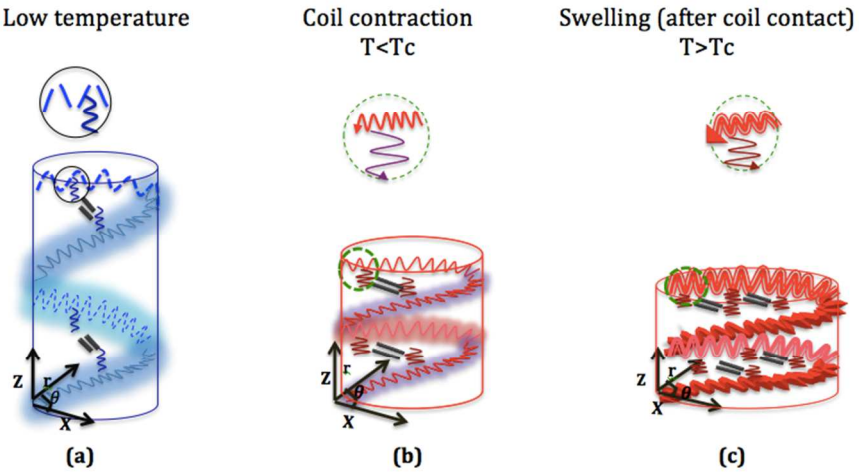

Fig. 2 Schematic represents the change in the molecular unit of the muscle when temperature fluctuates. Three configurations of muscle's chains have been shown: (a) the low temperature structure in which chains are in their fully extended configuration shown by dashed blue extended chains, (b) activated chains, before T_c (coil contact temperature), twist in helical path in which overall motion leads to shrinking in longitudinal direction and (c) saturated structure, after T_c, starts expanding in radial direction, graphed as thick double lines for intervening chains.

From macroscopic point of view, upon temperature rises, as shown in Fig. 3(b), the muscle contracts longitudinally. The red arrow is used to show the shrink initiation and propagation. At temperatures above coil's contact temperature (T_c), at which there is no room for the longitudinal contraction, muscle starts to expand radially and stiffening simultaneously. The schematic of the process has been depicted in Fig. 3(c).

Soft Matter Accepted Manuscript

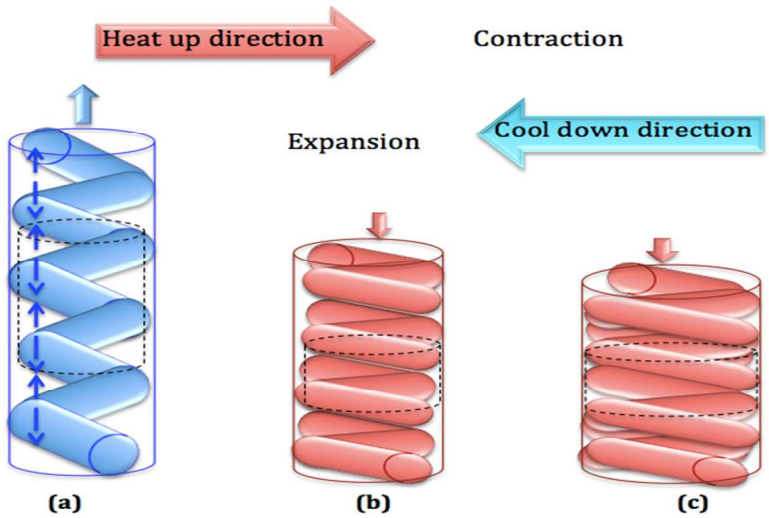

Fig. 3 The macroscopic structure evolution by temperature change in muscle has been shown in a three-step process (a) illustrates the room temperature state of muscle and active relaxation mechanisms, (b) indicates the contraction of the muscle after temperature increases and (c) illustrates the coils contact at T_c and radial expansion that occurs at the upper limit of muscle's contraction where there is no more room for longitudinal motion. The blue and red arrows have been used to show the direction of motion. The choice of color is based on temperature change; red for high temperature and blue for low temperature.

3. Model Description

In the sense of phenomenological formulation one may decompose the actuation response of the muscle into two elastic components that represent different thermal responses below and above the coil contact temperature T_c. The actuation strain tensor ${\varepsilon_{ij}}^t$ is given by

$${\varepsilon_{ij}}^t = \varepsilon_{ij}^{(1)} (1 - < T - T_c >) + \varepsilon_{ij}^{(2)} < T - T_c > \quad (1)$$

where $<>$ denotes Macaulay bracket, $\varepsilon_{ij}^{(1)}$ denotes strain response below T_c, called activated state strain hereinafter, and $\varepsilon_{ij}^{(2)}$ shows stain in saturated state which represents the system above T_c where coil contacts occur.

Fig. 4 demonstrates schematics of the proposed phenomenological model where the actuation strain is correlated to the thermal actuation. The *activated* and *saturated* states are represented by two sets of elastic springs. To model time dependent elastic deformation of the muscle system it is assumed that each state is constructed from a number of elastic springs that represent the individual molecular chains in each state. Below T_c the molecular chains are free to have longitudinal motion and their deformation results in $\varepsilon_{ij}^{(1)} = \sum_{k=1}^{N} \varepsilon_{ij}^{(1)k}$ where N denotes the number of chains and $\varepsilon_{ij}^{(1)k}$ is the strain due to longitudinal deformation in the k^{th} chain.

Once the temperature reaches to T_c, all molecular chains have reached to the full contact configuration, and they cannot have any longitudinal deformation. In this stage the active state must be switched to the saturated state in which the contacted coils undergo radial expansion that stiffens the muscle. Thus, in the saturated state, the *saturated chains* are responsible for

Soft Matter Accepted Manuscript

deformation mechanisms and they are modeled with a gradual activation of the structural switches in the saturated state. Thus, the saturated state's strain is given by $\varepsilon_{ij}^{(2)} = \sum_{k=1}^{N} \varepsilon_{ij}^{(2)k}$ where $\varepsilon_{ij}^{(2)k}$ shows the strain components for the k^{th} saturated chains. Two switches, shown in Fig. 4, are responsible to gradually exchange the muscle between activated and saturated states during heating or cooling processes.

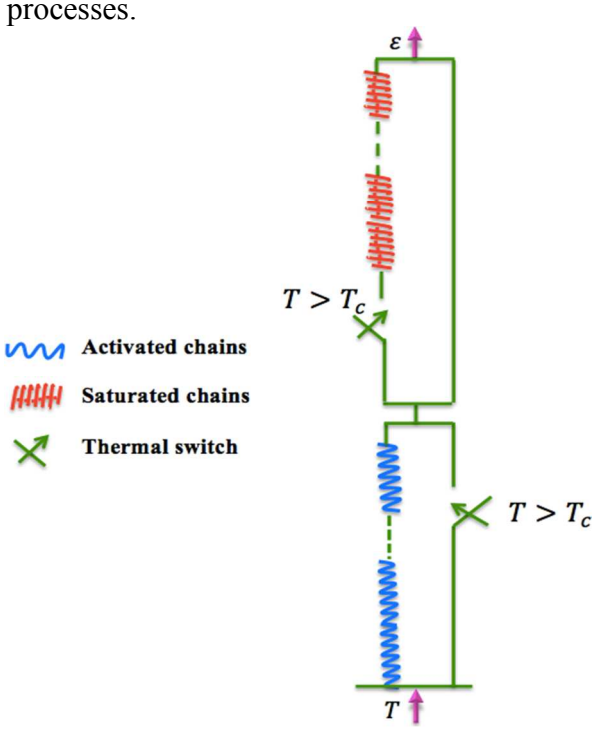

Fig. 4 1D analogy of the model for artificial muscle made of fishing line which shows two series of springs (each spring is a symbol of individual polymer chain) with a thermal switch in which heat flux activates springs one by one; this process is a temperature dependent process. Before T_c, both switches are open and the activated chains are responding to temperature change until muscle reach coil contact temperature (T_c). Coil contact temperature causes the activated chains to short circuit in a way that only saturated chains are responding to the temperature fluctuation.

In order to develop the constitutive model, it is assumed that the representative volume element (RVE) of the muscle is constructed from (a) k units of helically oriented chains, denoted by superscript h, and (b) l units of highly drawn chains, denoted by superscript d. The total number of chains in the unit volume of muscle is $N=k+l$. The volume fractions of helically oriented $\phi_h = k/N$ and highly drawn $\phi_d = l/N$ chains are linked together through the rule of mixture

$$\phi_h + \phi_d = 1 \qquad (2)$$

To bridge the microscale deformation mechanisms to the macroscopic deformation below T_c, it is assumed that the strain response for each molecular unit of chain obeys the rule of mixture

$$\varepsilon_{ij}^{(1)k} = \phi_h \varepsilon_{ij}{}^{(h)k} + \phi_d \varepsilon_{ij}{}^{(d)k} \qquad (3)$$

where $\varepsilon_{ij}{}^{(h)k}$ and $\varepsilon_{ij}{}^{(d)k}$represent the microscale strain tensors in k^{th} molecular unit due to the

Soft Matter Accepted Manuscript

twisting and drawing training processes, respectively. The macroscale strain tensor is then given by

$$\varepsilon_{ij}^{(1)} = \sum_{1}^{N} \varepsilon_{ij}^{(1)k} \tag{4}$$

Above T_c, only helically oriented chains in the saturated state contribute to actuation response while highly drawn chains are no longer active. Thus, the microscale strain tensor in each molecular unit is as follows

$$\varepsilon_{ij}^{(2)k} = \phi_h \varepsilon_{ij}{}^{(h)k} \tag{5}$$

where $\varepsilon_{ij}^{(2)k}$ denotes unit chain's strain tensor above T_c. The macroscopic strain above T_c is then given by

$$\varepsilon_{ij}^{(2)} = \sum_{1}^{N} \varepsilon_{ij}^{(2)k} \tag{6}$$

The switches in the model control the volume fractions and consequently the exchange between the two states occurs automatically. Fig. 5 shows the molecular unit, viz. microscopic RVE, and macroscopic RVE. The microscale and macroscale strains are schematically shown in Fig. 5.

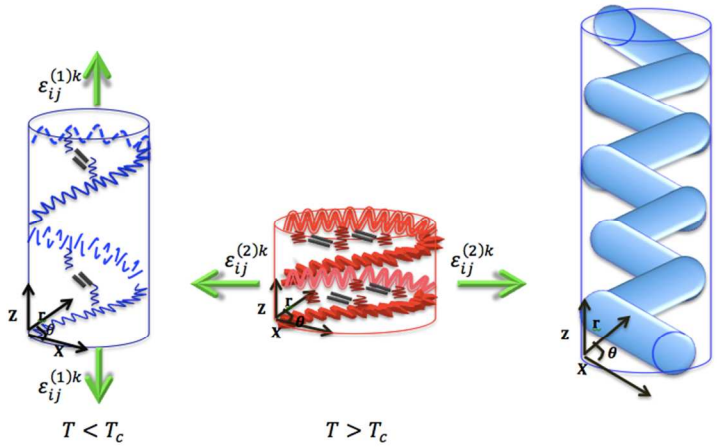

Fig. 5 (a) microscopic RVE below T_c, (b) microscopic RVE above T_c, and (c) Macroscopic RVE

The total macroscopic actuation strain is then correlated to the two activated $\varepsilon_{ij}^{(1)}$ and saturated $\varepsilon_{ij}^{(2)}$ strains in Eq. (1). Total stress is based on the linear elastic assumption written per Hooke's law as multiplications of effective stiffness L_{ijkl}^{e} and total strain $\varepsilon_{ij}{}^{t}$

$$\sigma_{ij}{}^{t} = L_{ijkl}^{e} \varepsilon_{kl}{}^{t} \tag{7}$$

with

$$L_{ijkl}^{e} = \phi_h L_{ijkl}^{h} + \phi_d L_{ijkl}^{d} \tag{8}$$

Soft Matter Accepted Manuscript

where L^h_{ijkl} and L^d_{ijkl} are stiffness tensors for twisted and drawn trained chains, respectively. To obtain the constitutive modeling the relation between thermal actuation and microscale level strains must be developed. Thermal actuation functions are defined to relate the macroscopic response to inherent properties of microscopic components namely helically oriented chains and highly drawn chains. The microscopic actuation strains due to drawn and twisting processes are defined by

$$\varepsilon_{ij}{}^{(d)k} = \alpha^{(d)}\Delta T \text{ , and } \varepsilon_{ij}{}^{(h)k} = \alpha^{(h)}\Delta T$$

where $\alpha^{(d)}$ and $\alpha^{(h)}$ are thermal actuation functions below and above T_c, respectively; and they are functions of molecular chains mechanical properties and also training cycles.

In other words, both fabrication and training processes have direct effect on moduli and actuation response of the molecular chains. This is in accordance with experimental observations in which muscles made of extra twisted insertion have higher load carrying capacity and higher actuation response. The effect of twist insertion has a direct correlation with stiffer helically oriented chains as a result of higher volume fraction of these chains, which leads to stiffer muscles. In order to formulate the dependence of the effective overall modulus on the drawn and twisted chains' volume fraction, one may assume

$$L^{(d)k}_{ijkl} = L^k_{ijkl} f\left(\varepsilon_{ij}{}^{(d)k}\right) \tag{9}$$

$$L^{(h)k}_{ijkl} = E^k g\left(\varepsilon_{ij}{}^{(h)k}\right) \tag{10}$$

where L^k_{ijkl} is un-trained molecule stiffness tensor, for the k^{th} chain, $L^{(d)k}_{ijkl}$ and $L^{(h)k}_{ijkl}$ are trained molecule stiffness tensors of k^{th} chain after drawing and twisting, respectively; and f and g are two material functions. To simplify the formulation process, the rule of mixture is used to define the overall effective modulus of the k^{th} chain as follows

$$L^{(e)k}_{ijkl} = \phi^k_h L^{(h)k}_{ijkl} + \phi^k_d L^{(d)k}_{ijkl} \tag{11}$$

where volume fractions of twisted ϕ^k_h and drawn ϕ^k_d chains in microscale are defined as follows

$$\phi^k_h = \left(\frac{\epsilon^{(h)k}_1}{\epsilon^{(h)k}_{max}}\right), \qquad \phi^k_d = \left(\frac{\epsilon^{(d)k}_1}{\epsilon^{(d)k}_{max}}\right) \tag{12}$$

where $\epsilon^{(d)k}_1$ and $\epsilon^{(h)k}_1$ denote respectively applied drawing and twisting strains during training cycle, and $\epsilon^{(d)k}_{max}$ and $\epsilon^{(h)k}_{max}$ are the maximum allowable drawn and twisting strains for k^{th} chain, respectively. $\epsilon^{(d)k}_{max}$ and $\epsilon^{(h)k}_{max}$ are two material parameters for the molecular chains that can be identified from experimental observations.

Soft Matter Accepted Manuscript

Statistical mechanics is utilized to model the physical behavior of the polymer chains. Gaussian distribution function has been used by Porter [16] and recently Shojaei and Li[17] to model the polymer mechanical responses. Following these works, two functions have been used to model physical behavior of the polymer chains during temperature variation (a) Gaussian distribution function, G_g, and (b) accumulative norm of G_g which is denoted by P_g [17].

$$\mathrm{G}_{\#}(\mathrm{T}, \mathrm{T}_{\#}, \sigma_{\#}) = \frac{1}{\sigma_{\mathrm{g}}\sqrt{2\pi}} \exp\left(-\frac{(\mathrm{T}-\mathrm{T}_{\#})^2}{2{\sigma_{\#}}^2}\right) \tag{13}$$

$$P_{\#} = \int_{\mathrm{T}_1}^{\mathrm{T}_2} (\mathrm{G}_{\#}(\mathrm{T}, \mathrm{T}_{\#}, \sigma_{\#})) = -\frac{1}{2}\,\mathrm{erf}\frac{(\mathrm{T}_{\#}-T)}{\sqrt{2}\sigma_{\#}} + \frac{1}{2} \tag{14}$$

where '#' is substituted by 'g' or 'c' to indicate glass transition and coil contact transition events, respectively; $\mathrm{T_g}$ here is the glass transition temperature of the muscle or the initial fiber and erf is the error function [18]. The standard deviation $\sigma_{\#}$ identifies half of the bandwidth for phase change during glass transition event. Based on a recent work by [17], the modulus has the following relation

$$\mathrm{E}' = \mathrm{E}'_0 \frac{1-\mathrm{P_c}}{1+\mathrm{P_c}} \tag{15}$$

where E'_0 (MPa) is a reference elastic tensile moduli at the low temperature, e.g. $\mathrm{T} = 25$ ℃. E'_0 should be defined in the numerical model to produce the obtained reference moduli from the DMA testing machine. In order to include the effect of various manufacturing and training parameters on the overall stiffness of the muscle Eq. (15) is further refined as follows

$$\mathrm{E} = \mathrm{E}' - \mathrm{CT} \tag{16}$$

where C is the muscle's spring constant and E′is the statistical elastic modulus, given in Eq. (15). In Eq. (16) the muscle's stiffness is assumed to have a linear dependency on spring constant C and also temperature T. It is shown that the proposed model correlated well with observed experimental data.

The actuation strain function is also temperature dependent and it is a function of muscle manufacturing and training cycle. The Gaussian distribution function has been used to formulate the actuation strain in which statistical mechanics provides a more physics based description for the chain actuation behavior. In order to include the manufacturing and training cycle in the actuation response, the effect of coiling has also been considered through material parameters α, β and γ. The actuation strain ε reads

$$\varepsilon = \alpha - \gamma\,\mathrm{T} - \beta.\,\mathrm{erf}\left(\frac{(-\mathrm{T_g}+\mathrm{T})}{\sigma_{\mathrm{g}}.\sqrt{2}}\right) \tag{17}$$

Based on a parametric study, presented in the results and discussion section, it is concluded that $\alpha \cong \beta$ and $\gamma \cong 10^{-4}\alpha$. Also parameters '$\alpha$' and '$\beta$' are directly related to the coil spring constant in which $\alpha \approx$5C to 6C with the muscle's spring index C=1.7.

The linear elasticity assumption for stress -strain is then applied to calculate the stress

Soft Matter Accepted Manuscript

$$\sigma = E.\varepsilon \quad (18)$$

where E and ε are given by Eqs. (16) and (17), respectively.

4. Numerical Framework

The constitutive model is numerically solved in MATLAB. In this section, the numerical implementation steps are elaborated and shown by a flow chart in Fig. 6. An artificial muscle with the highest spring constant, C = 1.7, found in the literature, is considered during implementation, while parametric study is also carried out to evaluate the effect of various parameters on muscle responses.

Fig. 6 shows the flowchart for the numerical implementation together with equation numbers and parameters used in each step. In this schematic, the process starts by obtaining the material properties from experimental graphs, which are listed in the first six columns of the Table 1. Determining design parameters, which meet the stress and strain requirements at critical transition temperature and relative duration of their structural change, are the main objective of our model. The last three parameters are defined to reduce the discrepancy between numerical model and experimental data. The least square approach has been utilized to calculate the error. This process continues until the amount of error in the numerical model reaches to 5% of experimental results. The effect of deviation from each material parameter is parametrically studied. The simulations are compared with the experimental results presented in10.

The error margin can be selected based upon the level of accuracy that is needed in a specific problem. In most engineering problems, 5% deviation provides an acceptable representation for the problem. In this work the least square method is used to find each of the three curve fitting parameters α, β, and γ. Ranges of these numerical parameters for having error less than 5% are as follows, 10 <α or β <10.2, and 0.000102< γ <0.00102. Figures 7-9 in the next section show the simulation results based on the given ranges of the material parameters, α, β, and γ, in which the deviation is less than 5%.

The numerical functions are defined and molded in a way to capture actual material response to temperature. In fact, these functions are applied to calculate the probability of activation of amorphous phase over working temperature and also estimate the saturation state of longitudinal motion at the coil contact temperature. They are defined based on probability density of the conformational evolution for the amorphous phase around critical temperatures (T_g or T_c). Therefore the Gaussian distribution probability (statistical mechanics) is considered as a building block of the current modeling process. As a matter of fact, the produced function integrates the change of internal parameters such as the coil angles, the number of twists, and the micro structural engineering process over working temperature by considering the probability of change of structure based on its macro-mechanical response.

Consequently, the modulus of the coiled muscle has been modeled using integration method over Gaussian distribution function; meanwhile, the strain function has been reproduced in the same procedure. The strain, which is the actuation function per percentage of the length as reported in the experiments, is a mechanical response of the artificial muscle; it indirectly

Soft Matter Accepted Manuscript

indicates the motion in the molecular length scale. This temperature dependent function implies the probability of conformational rotation and also chain stretching processes as temperature increases. The modeled modulus and strain functions have been used to calculate the stress response. Then the nominal stress versus tensile actuation within the temperature range has been plotted and compared with the experimental data.

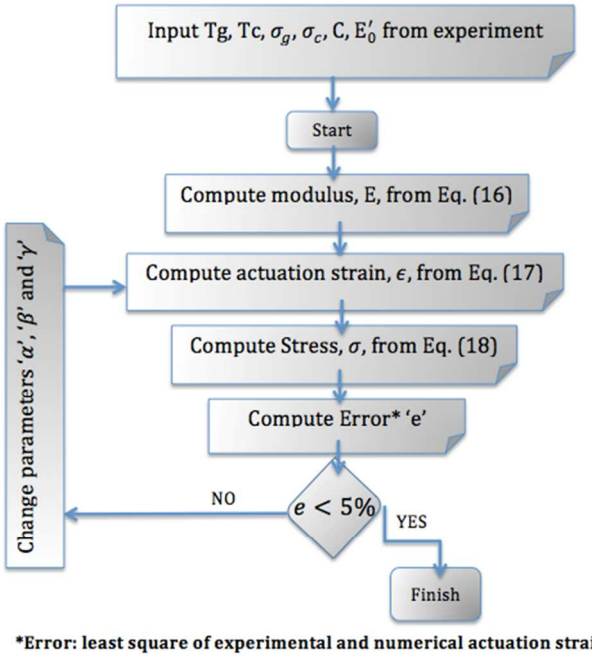

Fig. 6 Modeling process for artificial muscle made of fishing lines.

5. *Results and Discussions*

5.1 Determination of model parameters

In this section two types of material parameters have been introduced; the first type includes the first six parameters in Table 1; these parameters are indicated with asterisks in which they are directly imported from experimental results. The last three parameters indicating with Greek letters are determined from curve fitting efforts. Table 1 summarizes the material parameters used during the simulations.

Table.1 Material parameters used in the modeling

T_g(°C)*	T_c(°C)*	E_0'(MPa)*	σ_g(°C)*	σ_c(°C)*	C*	α	β	γ
90	130	1000	10	40	1.7	10.2	10.2	10.2×10^{-4}

*Obtained from experiments (Haines et al. 2014)

Three curve fitting parameters (α, β, γ) are introduced to mitigate deviation of numerical model. Consequently, the effect of these parameters on variation of the stress-strain numerical function has been studied. Variation in parameter 'α' results in change in terms of numerical stress-strain response as shown in Fig. 7. The numerical function is compared with the

Soft Matter Accepted Manuscript

experimental data and this graph shows that the best estimation for this parameter, is $\alpha \cong 5C$ to $6C$, with C=1.7. In fact, Parameter 'α 'defines vertical movement of the model with respect to experimental results.

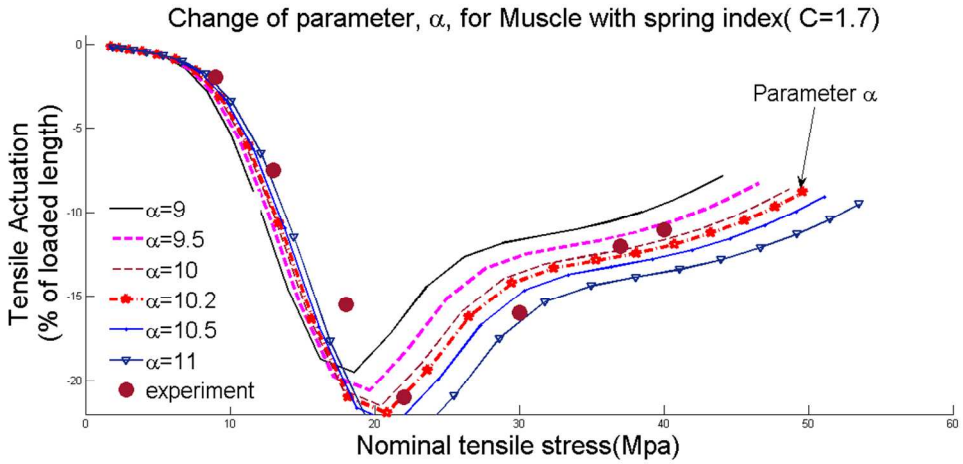

Fig. 7 Illustrates variations in stress-strain response with parameter '**α** ' in comparison with experimental results.

Parameter 'β' estimates the horizontal movement for the stress-strain numerical response versus experimental results. Fig. 8 shows that the parameter 'β' has the same value compared to parameter 'α '. However, this parameter is used to study the probability of the variation of model in the horizontal direction.

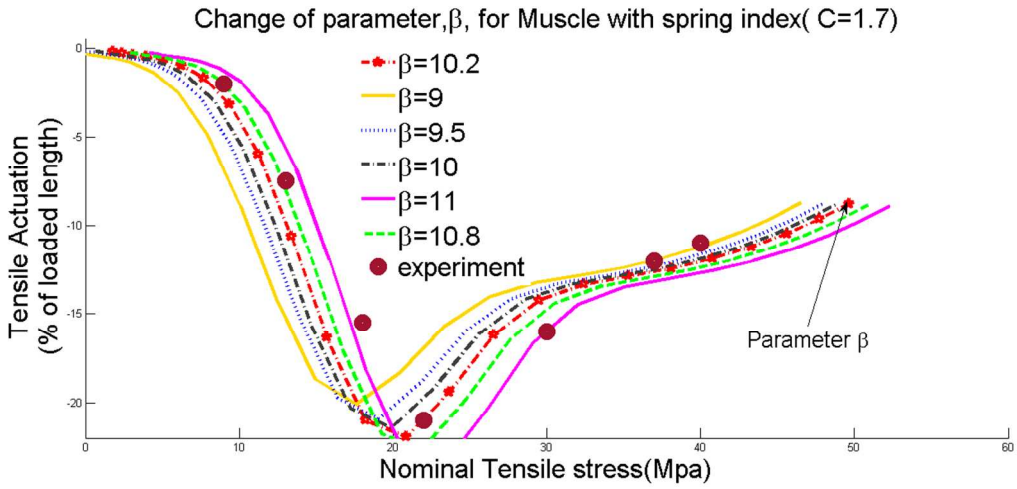

Fig. 8 Depicts fluctuations in stress-strain response with parameter, **β**, compared with experimental results.

Parameter γ is defined to add accuracy in muscle's stress-strain response. This parameter controls the span of the response. The optimal value for this parameter is $6 \times 10^{-4}C$, i.e., 0.000102, as shown in Fig. 9.

Soft Matter Accepted Manuscript

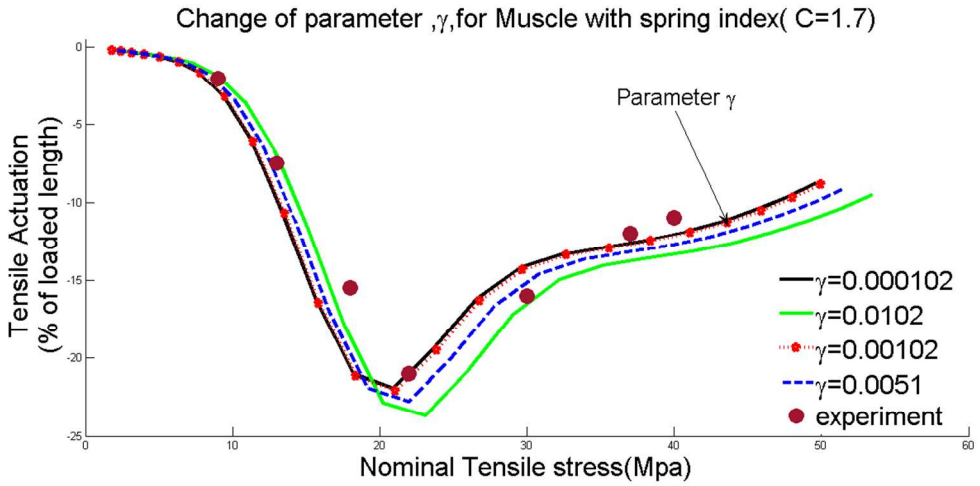

Fig. 9 Different stress-strain responses when parameter (γ) changes and these graphs are compared with experimental results.

5.2 Model validation and prediction

In this section the proposed formulation is numerically implemented and its performance is compared with the available experimental data from the literature. The numerical model is in a good agreement with experimental results.

Fig. 10 shows the variation of the muscle's modulus with respect to the temperature where Eq. (16) is used to plot this graph. It is worth noting that the material parameters T_c and σ_c are directly obtained from the experimental data and no curve fitting is required to plot this graph. Nominal elastic modulus is introduced in experimental results to address application of simple elasticity theory to calculate nominal stress and strain. Nominal stress (σ_N) at each cross section can be calculated by simply dividing the applied force by the initial cross-section area of the muscle. Also, nominal strain (ε_N) is defined as the amount of deformation normalized by the length, $\varepsilon_N = \frac{\Delta L}{L}$. Therefore, the nominal modulus can be defined as a fraction of nominal stress over nominal strain. The model's deviation from experiment can be managed by reduction in the effect of spring index and also by reducing the bandwidth of coil contact temperature. In this case, the amount of chains capable of fast responding to this transition would be reduced and the numerical graph would respond in a slower rate.

Soft Matter Accepted Manuscript

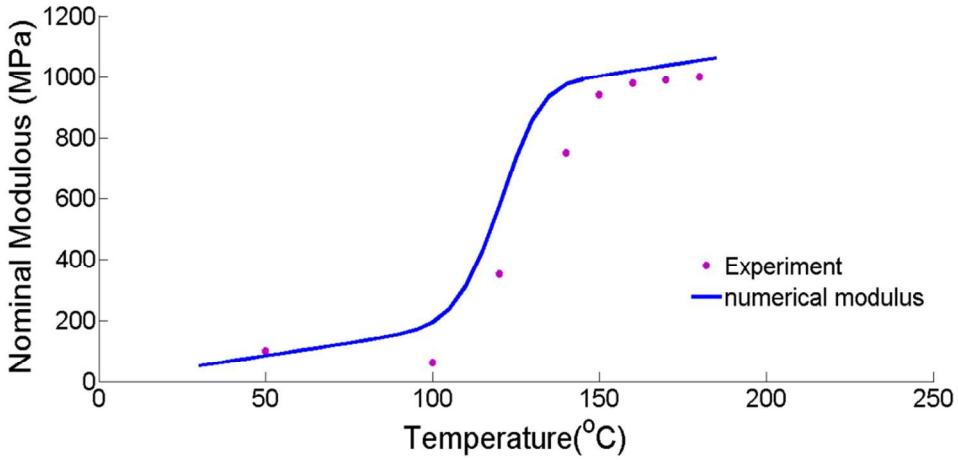

Fig. 10 The temperature dependence of the Modulus for Nylon 6.6 has been modeled mathematically and compared to the experimental results.

Fig. 11 depicts the actuation strain versus temperature in which Eq. (17) is used to plot this graph. This graph can be obtained directly from the experimental parameters by only knowing the magnitude of the spring index input as parameter α, however, the high degree of error resulted in definition of two other material parameters β, and γ. These parameters are numerically varied to achieve minimum deviation between simulation and experiment as it has been schematically presented in Fig. 6.

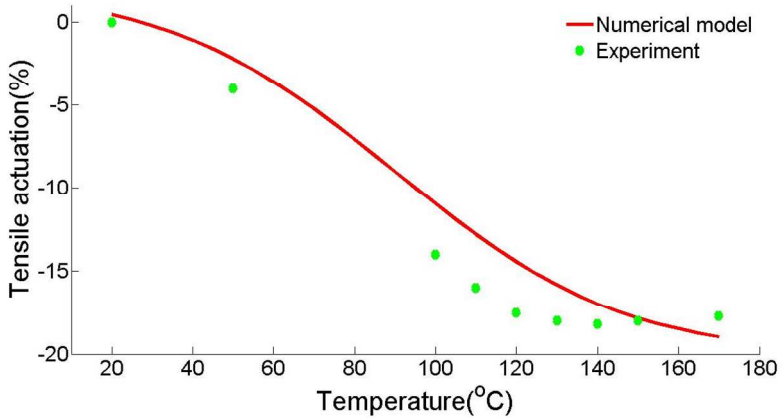

Fig. 11 The strain-temperature response of the muscle with spring constant C=1.7 has been modeled and compared to the experimental results.

The calibrated model is then used to plot stress actuation in Fig. 12 along with the corresponding experimental results. The model has acceptable agreement with experimental results for the constrained actuation response of the muscle, including the existence of a low peak that arises from the glass transition of the coiled fiber. Though the muscle becomes saturated in longitudinal direction when the coils contact, the thermal expansion becomes positive and the muscle expands radially in the range of 130℃ to 175℃.

Soft Matter Accepted Manuscript

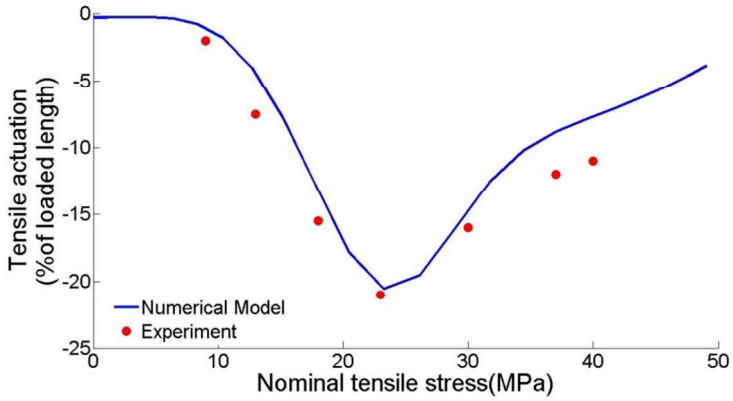

Fig. 12 The strain-stress recovery of the muscle with spring constant C=1.7 has been modeled and compared to the experimental results

In order to verify the capability of the proposed framework, in this section parametric study has been conducted and the results show that the proposed model can predict different muscles as depicted in Fig. 13. Three artificial muscles with different spring constants C=1.1, 1.4 and 1.7 have been plotted. Thorough scrutiny shows that the model can capture the trends and also the behavior of the experimental results.

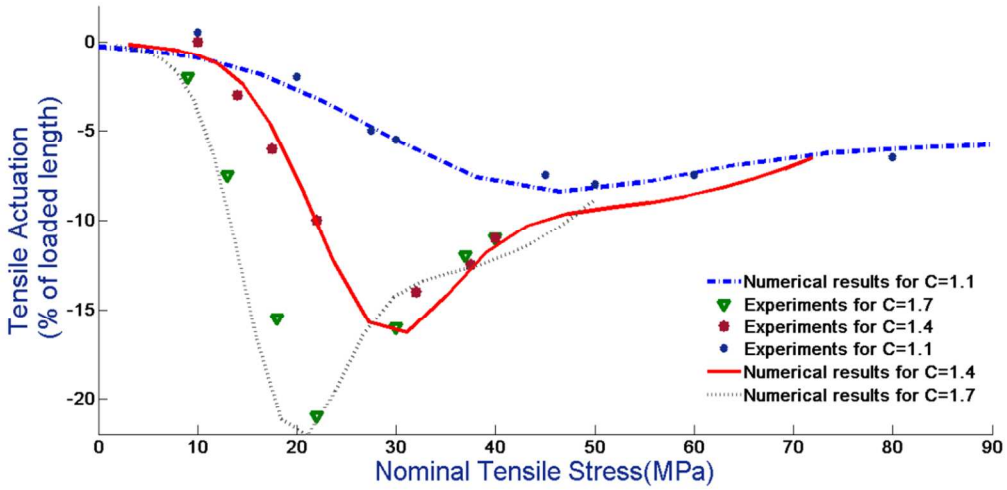

Fig. 13 Illustrations of the numerical simulation for three different muscles compared with their experimental results.

6. Conclusion

Skeletal muscles consist of bundles of twisted polymer fibers in which the integration of their motion enables us to lift loads in horizontal, vertical or even in twisted path. The current study may provide an interesting subject for further analysis in which mechanics of muscle structures can be incorporated into the modeling framework.

Artificial muscles are a new field of smart composite materials that are potentially applicable in different industries such as aerospace, robotic, biomedical, and self-healing [19-21]. In order to better design polymeric artificial muscles, it is highly desired to develop analytical and

Soft Matter Accepted Manuscript

numerical models [21]. In the current study, twisted and coiled Nylon 6.6 fibers are selected to fabricate an artificial muscle; these fibers are highly cold drawn before twisting. Micro-scale level of these muscles is controlled by engineering and training processes that provide two types of chains: (a) helically oriented chains that maintain a twisted shape in their training process and retrieve it during thermal actuation process; and (b) highly drawn chains that are able to actuate as soon as the muscle is heated up. However they saturate when coil contact temperature is reached.

Most previous modeling efforts in the case of artificial muscles concern different conceptual designs such as SMA or pneumatic muscles. Those models cannot simulate the twisting, coil contact, and transition events in twisted polymer based artificial muscles. The current modeling takes into account both polymer's nature as well as fabricating and training procedure of the artificial muscle made of polymer fiber. The proposed multiscale model is based on statistical mechanics of polymer chains in which several physical mechanisms are considered to develop the modeling framework.

The actuation response of the muscle is correlated to two basic molecular level deformation mechanisms that are longitudinal shrinkage of polymer chains and radial swelling due to thermal expansion. These microscale deformation mechanisms are linked to the macroscopic mechanical behavior through averaging techniques where a microscale RVE is bridged to the macroscale RVE. The thermal actuation response of the muscle over working temperatures has been scrutinized in the modeling section for both macro- and micro- scale response. Several design parameters such as manufacturing and training events are considered and their effects are coupled into the model.

Two categories of parameters are defined for estimation of the actuation response of the artificial muscle with temperature. Five parameters, viz. Tg, Tc, σc, σg, and C, are imported from experimental data to capture the effect of 1) critical temperature (Tg and Tc), 2) bandwidth for structural change during glass transition and coil contacts (σc and σg), and 3) macroscopic structure (spring index) of the muscle (C). The second categories of parameters, viz. α, β, and γ are numerically defined to estimate the molecular chain's rotation and expansion above coil contact temperature. Parameters α and β control the radial and angular deformation of the chains and parameter γ controls the deformation in the z direction. These three parameters, α, β, and γ, are interrelated and provide a good approximation to estimate the effect of temperature on the response of the artificial muscle. Their definition is basically commensurate to the training procedure for the artificial muscle.

It is shown that the proposed model is in good agreement with experimental results found in the literature. It is noted that the model is quite general. It may serve as a useful design and development tool for polymeric muscles with similar morphologies, such as Nylon, Polyethylene, shape memory Polyurethane fibers, etc., which are formed by twisting and coiling, and triggered by temperature rising.

Acknowledgment

This study was financially supported by National Science Foundation under grant number CMMI 1333997, the Cooperative Agreement NNX11AM17A between NASA and the Louisiana

Soft Matter Accepted Manuscript

Board of Re-gents under contract NASA/LEQSF(2011-14)-Phase3-05, and Army Research Office under grant number W911NF-13-1-0145.

References

1. Y. A. Ismail, J. G. Martínez, A. S. Al Harrasi, S. J. Kim and T. F. Otero. *Sensors and Actuators B: Chemical* 2011, 160, 1180-1190.
2. T. F. Otero and J. G. Martinez. *Sensors and Actuators B: Chemical* 2014, 199, 27-30.
3. G. Andrikopoulos, G. Nikolakopoulos and S. Manesis. *Control Engineering Practice* 2013, 21, 1653-1664.
4. H. Taniguchi. *APCBEE Procedia* 2013, 7, 54-59.
5. M. D. Lima, N. Li, M. Jung de Andrade, S. Fang, J. Oh, G. M. Spinks, M. E. Kozlov, C. S. Haines, D. Suh, J. Foroughi, S. J. Kim, Y. Chen, T. Ware, M. K. Shin, L. D. Machado, A. F. Fonseca, J. D. W. Madden, W. E. Voit, D. S. Galvão and R. H. Baughman. *Science* 2012, 338, 928-932.
6. T. V. Minh, B. Kamers, H. Ramon and H. Van Brussel. *Mechatronics* 2012, 22, 923-933.
7. Q. Zhao, D. Leon, A. David, B. Graham, and J.B. Markus. Biological materials by design. *Journal of Physics: Condensed Matter* 2014, 26, 073101.
8. Z. Qin, A. Fabre, and M.J. Buehler. *The European Physical Journal E* 2013, 36, 53.
9. J. Liu, J. Huang, T. Su, K. Bertoldi, and D.R. Clarke. *PLoS ONE* 2014, 9, e93183.
10. Z. Qin, and M.J. Buehler. *Physical Review Letters* 2010, 104, 198304.
11. C. S. Haines, M. D. Lima, N. Li, G. M. Spinks, J. Foroughi, J. D. Madden, S. H. Kim, S. Fang, M. Jung de Andrade, F. Goktepe, O. Goktepe, S. M. Mirvakili, S. Naficy, X. Lepro, J. Oh, M. E. Kozlov, S. J. Kim, X. Xu, B. J. Swedlove, G. G. Wallace and R. H. Baughman. *Science* 2014, 343, 868-872.
12. G. Genuini, G. Casalino, P. Chiarelli and D. De Rossi. in *Kinematic and Dynamic Issues in Sensor Based Control,* ed. G. Taylor, Springer Berlin Heidelberg 1990, 57, 341-360.
13. C.-P. Chou and B. Hannaford. *Robotics and Automation, IEEE Transactions on* 1996, 12, 90-102.
143. A. Sung-Min, R. Junghyun, C. Maenghyo and C. Kyu-Jin. S*mart Materials and Structures* 2012, 21, 055009.
15. K. K. Şafak and G. G. Adams. Robotics and Autonomous Systems 2002, 41, 225-243.
16. D. Porter. *Group Interaction Modelling of Polymer Properties*, Taylor & Francis, 1995.
17. A. Shojaei and G. Li. *Proceedings of the Royal Society A: Mathematical, Physical and Engineering Science* 2014, 470, 20140199.
18. E. W. Weisstein. *MathWorld--A Wolfram Web Resource*. 2014.
19. A. Shojaei, S. Sharafi and G. Li. *Mechanics of Materials* 2015, 81, 25-40.
20. G. Li. *Self-healing composites: shape memory polymer based structures*, John Wliey & Sons, Inc., 2014.
21. A. Shojaei and G. Li. *International Journal of Plasticity* 2013, 42, 31-49.

Soft Matter Accepted Manuscript